JOURNAL OF PHYSICAL ORGANIC CHEMISTRY
J. Phys. Org. Chem. 2005; **18:** 62–68
Published online 6 July 2004 in Wiley InterScience (www.interscience.wiley.com). DOI: 10.1002/poc.771

DFT study of the mechanism of nitration of toluene with nitronium

Litao Chen,[1,2] Heming Xiao[1]* and Jijun Xiao[1]

[1]Department of Chemistry, Nanjing University of Science and Technology, Nanjing 210094, China
[2]Institute of Chemical Engineering, Zhejing University of Technology, Hangzhou 310014, China

Received 14 October 2003; revised 23 December 2003; accepted 11 January 2004

ABSTRACT: Reaction profiles of the isomeric nitration of toluene with nitronium ion were studied. Stationary points including three isomeric transition states were successfully located and characterized for the first time by employing hybrid DFT procedures at the B3LYP/6–311G** level without any restriction on the internal coordinates. Further correlation energy corrections by MP2/6–311G**//B3LYP/6–311G** were performed to evaluate the activation barrier heights. Mechanistic studies on the geometry, charge, energy and IR spectrum of the stationary points were carried out to illustrate the microscopic nitration process. A comparison of the nitrations of toluene and benzene shows that the methyl group plays dual roles in the nitration of toluene for its inductive and superconjugative effects. That is, the introduction of a methyl group creates favorable sites for the attacker and stabilizes the isomeric toluene–NO_2^+ complexes. Both roles are critical to the positional selectivity. The order of the activation barrier height is *para* < *ortho* < benzene < *meta*. This relative reactivity order is not changed with either B3LYP/6–311G** or MP2/6–311G**//B3LYP/6–311G** calculations, although the absolute magnitude of the latter is larger. The order of the stability of complexes is *p*-toluene–NO_2^+ > *o*-toluene–NO_2^+ > *m*-toluene–NO_2^+ > benzene–NO_2^+. The relationship between the energy and the electron migration of NO_2 group was established to elucidate the stabilization caused by the interaction between the two moieties of the complex. The vibrational shifts of tetrahedral C—N and C—H bonds suggest that the nitration of toluene may undergo the classical electrophilic substitution pathway, namely an S_E2 mechanism. Copyright © 2004 John Wiley & Sons, Ltd.

KEYWORDS: toluene; DFT; nitration mechanism; selectivity

INTRODUCTION

Electrophilic aromatic substitution is one of the most thoroughly studied reactions in organic chemistry owing to its wide range of applications from medicines to dyes and explosives. Many theories have been extensively developed in this field. However, the mechanism of aromatic nitration continues to be the subject of active research and some controversy.[1–11] A problem in theoretical studies is the lack of the fully optimized structure of transition state(s) on the profile of aromatic nitrations.[4–9] Politzer *et al.*[5] calculated the properties of some possible intermediate stages for the nitrations of benzene and toluene at HF/STO-6G and HF/5–31G levels by freezing both N—O bond lengths of NO_2^+. Yet no connections, in terms of pathway, were involved for these complexes. In 1992, Szabo *et al.*[9] finally obtained two energy profiles for the nitration of benzene with the possible protonated methyl nitrate isomers also by incomplete optimization. For the case of benzene with bare (unsolvated) nitronium ion, however, no activation barrier was found along the chosen reaction coordinate.

Continuing our interest in nitro compounds as important energetic materials, we embarked on a study of the aromatic nitration mechanism. Benzene and toluene are well-known basic units to build up high-energy polymeric materials. Recently, we reported our findings concerning the nitration of benzene with nitronium ion.[12] The results of theoretical calculations at the B3LYP/6–311G** level[13–15] were in good agreement with the experimental observations and provided explicit explanations for the isotope effect and the influence of the reaction medium. As a continuation, we extended our investigation to the toluene system. It is hoped that this will provide a better understanding of the positional selectivity of electrophilic substitution through comparative and systematic investigations on the isomeric nitration of toluene.

COMPUTATIONAL ASPECTS

Whereas the conventional *ab initio* method at the Hartree–Fock level shows large errors for the nitro

**Correspondence to:* H.-M. Xiao, Department of Chemistry, Nanjing University of Science and Technology, Nanjing 210094, China.
E-mail: xiao@mail.njust.edu.cn
Contract/grant sponsor: National Natural Science Foundation of China; *Contract/grant number:* 20173028.

group-containing system (see above), the DFT procedures appear to behave well,[16–21] with no major failures of the theory. Therefore, B3LYP/6–311G** procedures were employed here to calculate the isomeric nitration trajectories of toluene. Stationary points were all fully optimized without any restriction on the internal coordinate. Harmonic vibrational frequency analysis was calculated at the same level to characterize each stationary point. The -reactant complex (σ-R) and Wheland intermediate[2] (σ-INT) gave only real frequencies. And the σ-transition-state complex (σ-TS) was identified as a first-order saddle point by its only one imaginary frequency. Tight convergence criteria were used for the optimization of the transition state (TS) owing to the flat potential of the nitro group-containing ring system.[9,10] Since three isomeric additions were involved in the nitration of toluene and each has three stationary points of reactant (R), transition state (TS) and intermediate (INT) on its own energy profile, a total of nine stationary points were located and characterized at the B3LYP/6–311G** level. For a better evaluation of the activation height, further correlation energy correction by MP2 with the same basis set was performed at the B3LYP-optimized geometry for the stationary points of σ-R and σ-TS. All the calculations were performed using the Gaussian 98 program package[22] on a α-workstation.

RESULTS AND DISCUSSION

Since the classical studies of Ingold and co-workers,[1] it has been generally accepted that the nitrating agent is usually the nitronium ion, NO_2^+, and the primary addition step to form a σ-complex, called a Wheland intermediate, is the rate-limiting step. Therefore, we focused our attention on the first addition step without involving the second (fast) proton elimination step. As a continuation of the benzene case, the substituent effects on the benzene ring and the consequent positional selectivity were our central task here.

In the benzene case, two transition states were found as NO_2^+ approaches benzene along the reaction coordinate. The first to appear is a bridge π-TS, in which the distances between the nitrogen atom of the nitronium ion to both carbon atoms C_1 and C_6 of the benzene ring were equal. It acts like a bifurcation point which shifts the positive ion to either single carbon C_1 or C_6 to form σ-R. The energy barrier for the conversion is small, only 2.355 kJ mol^{-1}. The reason for the formation of π-TS is that the highly uniform π bonds above and below the benzene plane make the NO_2^+ first approach not a single carbon, but the π-electron region between two carbon atoms. In toluene, however, the π electrons could not be as uniform as in benzene. They redistribute to different sites by different populations under the influence of the incoming methyl group. Therefore, no such isoceles triangle π complex can be found when NO_2^+ attacks toluene. Only three stationary points, σ-R, σ-TS and σ-INT, were included in the first addition step of the nitration of toluene.

One common phenomenon found in the toluene case is that the formation of the tetrahedral C—N bond and the cleavage of the tetrahedral C—H bond were also not concerted, but stepwise in the process of the nitration. This reflects the fact that the experimental observation of the absence of a kinetic isotopic effect is not only found in benzene nitration, but also in most aromatic nitrations.[23,24]

In order to determine how and to what extent the methyl group would impact the aromatic ring in the concerned rate-limiting step, we discuss the following properties by a comparison of the nitrations of toluene and benzene.

Geometries

The carbon atom C_1 is appointed the attacked carbon by NO_2^+. The methyl group belongs to C_2 in the *ortho* σ complex, but shifts to C_3 in the *meta* and to C_4 in the *para* σ complex, respectively. The five hydrogen atoms 8–12 are linked to the ring carbons in a clockwise manner. The hydrogens H_{13} to H_{15} belong to the methyl group. The notation for the *ortho* σ complex is shown in Fig. 1 as an example. Some key geometric parameters and bond orders for each optimized structure are given in Table 1.

As can be seen in Table 1, the C—C bond length within the ring shows that these nine σ complexes are in a remarkably consistent skeleton pattern. This kind of resonance structure we also found in the benzene case. In those complexes, the tetrahedral C—C bonds (C_1—C_2, C_1—C_6) are the longest, whereas those next to them (C_2—C_3 and C_5—C_6 bonds) are the shortest, regardless of the location of the methyl group.

The C—C bond length of ethane is 153.1 pm by calculation at the same level. The C—C_7 bond length in toluene, however, is 151.0 pm. This is obviously due to the hyperconjugation between the methyl group and the ring. It becomes even shorter when NO_2^+ arrives (see Table 1).

The NO_2 group is located at a single carbon atom and is no longer linear in each σ complex. The N—O bond lengthens and the O—N—O angle diminishes, and it

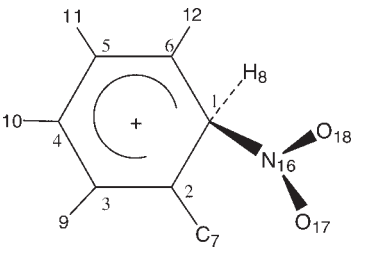

Figure 1. The notation of atoms

Table 1. Characteristic geometric parameters and bond orders for stationary points of toluene nitration[a]

	σ-R			σ-TS			σ-INT			
Parameter[b]	*o*	*m*	*p*	*o*	*m*	*p*	*o*	*m*	*p*	SR[c]
$r(C_1—N_{16})$	197.1	210.0	193.9	166.9	178.9	174.1	162.2	160.6	159.9	
$r(C_1—H_8)$	108.4	108.3	108.3	109.5	109.1	108.9	110.3	111.2	110.8	108.6
$r(C—C_7)$	148.8	150.1	148.5	148.1	150.5	148.1	148.3	150.4	148.1	151.0
$r(C_1—C_2)$	146.0	142.6	144.6	149.4	146.0	146.7	149.0	146.8	147.2	139.9
$r(C_2—C_3)$	138.8	137.9	136.4	138.3	137.6	136.2	138.1	137.3	135.9	139.9
$r(C_3—C_4)$	139.5	142.5	142.5	139.7	141.7	142.3	140.0	142.0	142.6	139.3
$r(C_4C_5)$	142.1	140.0	142.3	142.1	141.4	143.0	141.7	141.0	142.6	139.3
$r(C_5C_6)$	136.5	137.8	136.5	135.5	136.4	135.7	135.9	136.6	135.9	139.3
$r(C_6C_1)$	143.9	143.9	144.7	147.6	145.5	146.3	147.8	146.6	147.2	139.3
$r(N_{16}—O_{18})$	118.1	117.3	118.1	119.9	118.9	119.2	120.3	120.3	120.4	119.8
$\alpha(O_{17}N_{16}O_{18})$	136.2	139.1	135.7	129.8	133.1	132.0	129.4	129.6	129.3	180.0
$\alpha(N_{16}\,C_1H_8)$	95.7	94.3	96.0	99.7	95.9	98.4	99.7	98.9	99.5	
$\beta(O_{18}N_{16}C_1H_8)$	18.3	−12.8	−2.4	49.0	43.4	31.9	−59.0	−87.3	−88.7	
Bo[d] $(C_1—N_{16})$	0.158	0.131	0.154	0.154	0.154	0.161	0.152	0.129	0.136	
Bo[d] $(C_1—H_8)$	0.416	0.410	0.405	0.388	0.391	0.396	0.358	0.340	0.348	0.417
Bo[d] $(C—C_7)$	0.341	0.338	0.346	0.330	0.336	0.346	0.329	0.330	0.343	0.360

[a] Bond lengths in pm and angles in degrees.
[b] See Fig. 1 for notation of atoms.
[c] Separated reactants: toluene and nitronium ion.
[d] Bond order.

approaches closer to the C_1 atom on going from σ-R to σ-TS, and to σ-INT in any of the pathways of *ortho*, *meta* or *para* attack.

The distance between the nitrogen atom of the nitronium ion and the attacked carbon atom, $r(C_1—N_{16})$, was chosen as the reaction coordinate. In the σ-TS of *o*-toluene–NO_2^+, it is 'abnormally' short, 166.9 pm, suggesting that the transition state is likely to be a 'late' TS. This means that its configuration is closer to the σ-INT than to the σ-R complex. $r(C_1—N_{16})$ of σ-*ortho*-INT is 162.2 pm, longer than that of the other two Wheland intermediates (*meta*-*ortho*-INT and *para*-*ortho*-INT), owing to the steric interaction between the methyl and the nitro groups, especially in a close vicinity.

The tetrahedral $C_1—H_8$ bond lengthens whereas the corresponding bond order decreases on going from σ-R to σ-TS to σ-INT. However, the variation either in the $C_1—H_8$ bond length or in its bond order is not drastic. This means that the cleavage of $C_1—H_8$ would not occur in the primary rate-determining addition step, consistent with the experimental observation of the absence of a kinetic isotope effect in most aromatic nitrations.

Charges

The electrophilic agent NO_2^+ is electron deficient and therefore has a strong driving force to interact with electron-rich aromatics. Hence it is important to recognize how and to what extent the charge has migrated from one moiety to the other in the process. The charges of atoms, concerned groups and separated reactants are given in Table 2. The total charge density of *p*-toluene–NO_2^+ complexes of σ-R, σ-TS and σ-INT are shown in Fig. 2 as an example of isomeric substitutions of toluene with nitronium ion.

The charge of the methylated carbon (C_2) in toluene is −0.1027 e, more negative than that in benzene, −0.0945 e. This charge redistribution shows up the inductive and hyperconjugative effects of the methyl group upon the aromatic ring.

Comparing the atomic charge in the three σ-R complexes with that in the free toluene molecule, one can see that a significant electronic charge moves from the hydrogens, both of the aromatic ring and of the methyl group, to the attacked carbon (C_1). Hence the hydrogen atoms are the source of electronic charge, under the stimulus of the strong electron-withdrawing power of the nitro group.

As seen in Table 1, the charge of the nitro group of the three isomeric σ-R complexes is 0.169, 0.249 and 0.144 e for *ortho*, *meta* and *para* substitution, respectively. This obviously follows the order *meta* ≫ *ortho* > *para*. The C_1–N distance of the three isomeric σ-R complexes is 197.1, 210.0 and 193.9 pm, respectively, and also follows the order *meta* > *ortho* > *para*. This implies that the *meta* position is the least favorable site for attack. With respect to the corresponding results for benzene, 0.273 e and 209.7 pm, the above two orders should be benzene > *meta* ≫ *ortho* > *para* and *meta* > benzene > *ortho* > *para*, respectively. The former order explicitly shows that more electronic charge has migrated from the aromatic ring to the nitro group at the stage of forming the σ-R complex in the isomeric nitrations of toluene than in the nitration of benzene, especially in the *ortho* and *para* nitrations of toluene.

Since there are two *ortho* but only one *para* position in the monosubstituted aromatic ring, an *ortho*:*para* ratio of

Table 2. Mulliken net charges[a] and dipole moments[b] for stationary points of toluene nitration

	σ-R			σ-TS			σ-INT			
	o	*m*	*p*	*o*	*m*	*p*	*o*	*m*	*p*	SR
C_1	−0.284	−0.266	−0.268	−0.165	−0.224	−0.207	−0.115	−0.110	−0.103	−0.075
C_2	0.006	0.062	0.057	−0.019	0.068	0.044	−0.050	0.024	−0.006	−0.103
C_3	−0.043	−0.128	−0.051	−0.011	−0.116	−0.019	−0.010	−0.109	−0.011	−0.075
C_4	0.011	0.022	−0.037	−0.005	0.020	−0.061	−0.007	0.023	−0.070	−0.093
C_5	−0.076	−0.064	−0.050	−0.038	−0.044	−0.018	−0.041	−0.038	−0.011	−0.094
C_6	0.059	0.031	0.057	0.012	0.030	0.027	0.004	0.002	−0.006	−0.093
C_7	−0.224	−0.243	−0.246	−0.225	−0.240	−0.247	−0.240	−0.239	−0.247	−0.259
H_8	0.209	0.204	0.212	0.246	0.247	0.237	0.261	0.272	0.265	0.083
ΣH_{ring}	0.670	0.663	0.662	0.702	0.709	0.686	0.725	0.754	0.727	0.358
ΣH_{sub}	0.503	0.471	0.521	0.527	0.479	0.537	0.532	0.487	0.543	0.351
N_{16}	0.338	0.366	0.334	0.287	0.308	0.296	0.281	0.284	0.280	0.783
O_{18}	−0.082	−0.055	−0.085	−0.154	−0.114	−0.128	−0.164	−0.175	−0.180	0.108
NO_2	0.169	0.249	0.144	−0.024	0.071	0.021	−0.060	−0.065	−0.080	1.000
Dipole	2.757	1.542	2.896	5.432	4.162	4.926	5.936	6.107	6.790	0.352

[a] Charges in electron units.
[b] Dipole moments in debye.

2:1 should be expected statistically. However, the steric hindrance of the *ortho* orientation makes the *para* position the most favorable site to the attack, so the *ortho* : *para* ratio is diminished to $\sim$1.57.

Although the dipole moment of benzene is zero, that of toluenes is 0.352 D (see the last row of Table 2). The weakly electron-donating effect of the methyl group is obviously responsible for the appreciable dipole moment of toluene. As also seen in the last row of Table 2, the dipole moment of σ complex increases more or less progressively along the reaction coordinate from σ-R to σ-TS to σ-INT for either *ortho*-, *meta*- or *para*- substitution. This means that the closer the nitronium ion approaches the ring, the higher the polarization of the σ complex will generally be.

Energetics

The stabilization energy of the σ complex is defined as $\Delta E_{stab} = E_{complex} - (E_{aromatic\ molecule} + E_{NO_2^+})$. For three loose isomeric σ-Rs of toluene–NO_2^+, their stabilization energies are −157.6, −147.0 and −163.3 kJ mol^{-1} for *ortho*, *meta* and *para* substitution, respectively. This demonstrates that there is a great driving force for the initial pair of aromatic molecule and nitronium ion to

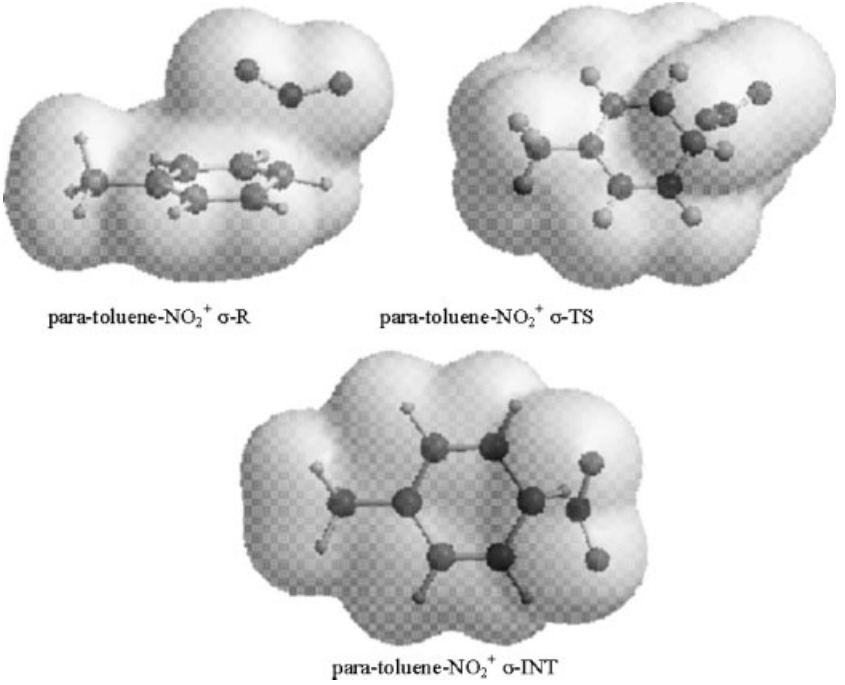

Figure 2. Calculated total charge density of *p*-toluene–NO_2^+ σ-R, σ-TS and σ-INT complexes at the B3LYP/6–311G** level

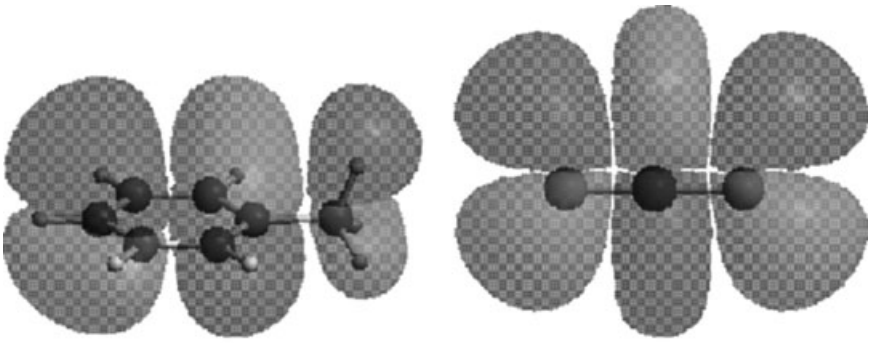

Figure 3. Calculated FMO diagrams of separated reactants at the B3LYP/6–311G** level

form an electron donor–acceptor (EDA) complex. The calculated FMO diagrams of separated reactants are shown in Fig. 3. The symmetry of both the HOMO and LUMO orbitals suggests that the formation of the EDA complex is a kind of typically allowed reaction. With respect to the stabilization energy of the corresponding benzene case, $-130.4\,\mathrm{kJ\,mol^{-1}}$, the order of the stability of σ-R is *para* > *ortho* > *meta* > benzene, consistent with that of charge migration from aromatics to the nitro group. Since this order is the reverse of the order of the charge left on NO_2 group at the σ-R stage, 0.144 (*para*) < 0.169 (*ortho*) < 0.249 (*meta*) < 0.273 (benzene) (see above). This implies that the electron-donating methyl group promotes the charge migration and is, at least partly, responsible for the stabilization of toluene–NO_2^+ σ complexes.

The relative energy of isomeric complexes in Table 3 could be delineated as in Fig. 4 with respect to the benzene case. The relative energy [$E_R(Z)$] of the Wheland intermediate here is actually the reaction heat of the rate-limiting step. From the viewpoint of thermodynamics, this heat is correlated to the stability of Wheland intermediates. From the reaction heat of the three toluene–NO_2^+ intermediates, one can see that only the *para* electrophilic addition is exothermic, and thus energetically feasible. The *ortho* site addition, however, is the least feasible, mainly owing to its steric crowding.

In order to evaluate the impact of the methyl group on the aromatic ring, we define the isodesmic energy as $\Delta E_i = \Delta E_{stab}$ (toluene–NO_2^+) − ΔE_{stab} (benzene–NO_2^+) to calculate the extra stabilization energy caused by methyl group for all the toluene–NO_2^+ complexes, shown in the last row of Table 3. These negative values demonstrate that the methyl group does stabilize the toluene–NO_2^+ complex by its inductive and hyperconjugative effects. Comparing the isodesmic energies for each column of σ-R, σ-TS and σ-INT, the stability order by substitution sites is *para* > *ortho* > *meta* for either the σ-R, σ-TS or σ-INT stationary point. This is consistent with the corresponding order by the FMO energy gaps, implying that the energy gap of HOMO and LUMO could also indicate the stability of isomeric complexes to a certain extent.

Kinetically, the activation energy order *meta* ($9.481\,\mathrm{kJ\,mol^{-1}}$) > benzene ($8.370\,\mathrm{kJ\,mol^{-1}}$) ≫ *ortho* ($4.776\,\mathrm{kJ\,mol^{-1}}$) > *para* ($2.581\,\mathrm{kJ\,mol^{-1}}$) (see Fig. 4) reflects the reaction activity of the nitrations of benzene and isomeric toluene. In order to evaluate the activation

Table 3. Energies for stationary points of toluene nitration

	σ-R			σ-TS			σ-INT		
	o	*m*	*p*	*o*	*m*	*p*	*o*	*m*	*p*
$E(T)$[a]	−476.47160	−476.46729	−476.47357	−476.46965	−476.46360	−476.47237	−476.47163	−476.46682	−476.47575
$E(Z)$[a,b]	−476.33163	−476.32761	−476.33380	−476.32981	−476.32400	−476.33282	−476.33149	−476.32695	−476.33594
$E_R(Z)$[b,c]	0.0	0.0	0.0	4.776[f]	9.481[f]	2.581[f]	0.3623	1.7302	−5.6186
HOMO[c]	−1198.2	−1182.6	−1226.2	−1227.6	−1212.0	−1240.1	−1239.1	−1236.3	−1246.5
LUMO[c]	−876.4	−895.7	−867.4	−881.5	−893.8	−870.0	−871.3	−883.3	−860.2
GAP[c,d]	321.8	286.9	358.7	346.1	318.2	370.1	367.8	353.0	386.3
$\Delta E_i(Z)$[b,c,e]	−27.13	−16.58	−32.84	−30.73	−15.47	−38.63	−29.12	−17.20	−40.81

[a] Energies in hartree.
[b] Corrected for ZPVE.
[c] Energies in $\mathrm{kJ\,mol^{-1}}$.
[d] Energy gap of LUMO and HOMO.
[e] Isodesmic energy defined by the equation $\Delta E_i = E_{benzene} - E_{toluene} + E_{toluene-NO_2^+} - E_{benzene-NO_2^+}$.
[f] Activation energies.

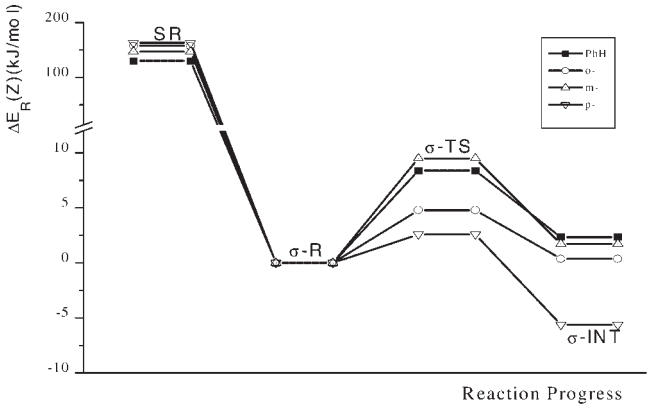

Figure 4. Energy profiles for the nitration of benzene and toluene with nitronium at the B3LYP/6–311G** level

barrier heights precisely, a further correlation energy correction by MP2 with the same basis set was performed at the B3LYP-optimized geometry of reactants and transition states. The modified activation energies are 53.66 kJ mol^{-1} for *meta* substitution, 52.56 kJ mol^{-1} for benzene, 31.56 kJ mol^{-1} for *ortho* substitution and 21.79 kJ mol^{-1} for *para* substitution. The absolute value of the activation energy is increased, but the relative magnitude is kept in the same order as mentioned above, *meta* > benzene ≫ *ortho* > *para*. This implies that the absolute value of the activation energy is dependent on the computational method employed. The activation order suggests the well-known *ortho*, *para*-directing property of the methyl group. That is, the *para* and *ortho* sites are highly activated, but the *meta* sites are deactivated, by the methyl group.

Overall, it is evident that the *para* site is the most favorable and the *meta* is the least favorable, consistent with the experimental isomer distribution in the nitration of toluene.

IR spectra

B3-based DFT procedures are routinely used to give accurate estimates of experimental fundamentals.[25,26] The following harmonic vibrational frequencies are provided by these very cost-effective means. The calculated vibrational frequencies of the four complexes presented here were not scaled because the B3 exchange functional yields scaling factors very close to unity and could therefore often be used directly without resorting to frequency scailing.[27]

For the Wheland intermediates experimentally available, the IR spectra of the three isomeric σ intermediates are presented in Fig. 5. For comparative purposes, the infrared spectrum of the *ortho* transition state is also shown.

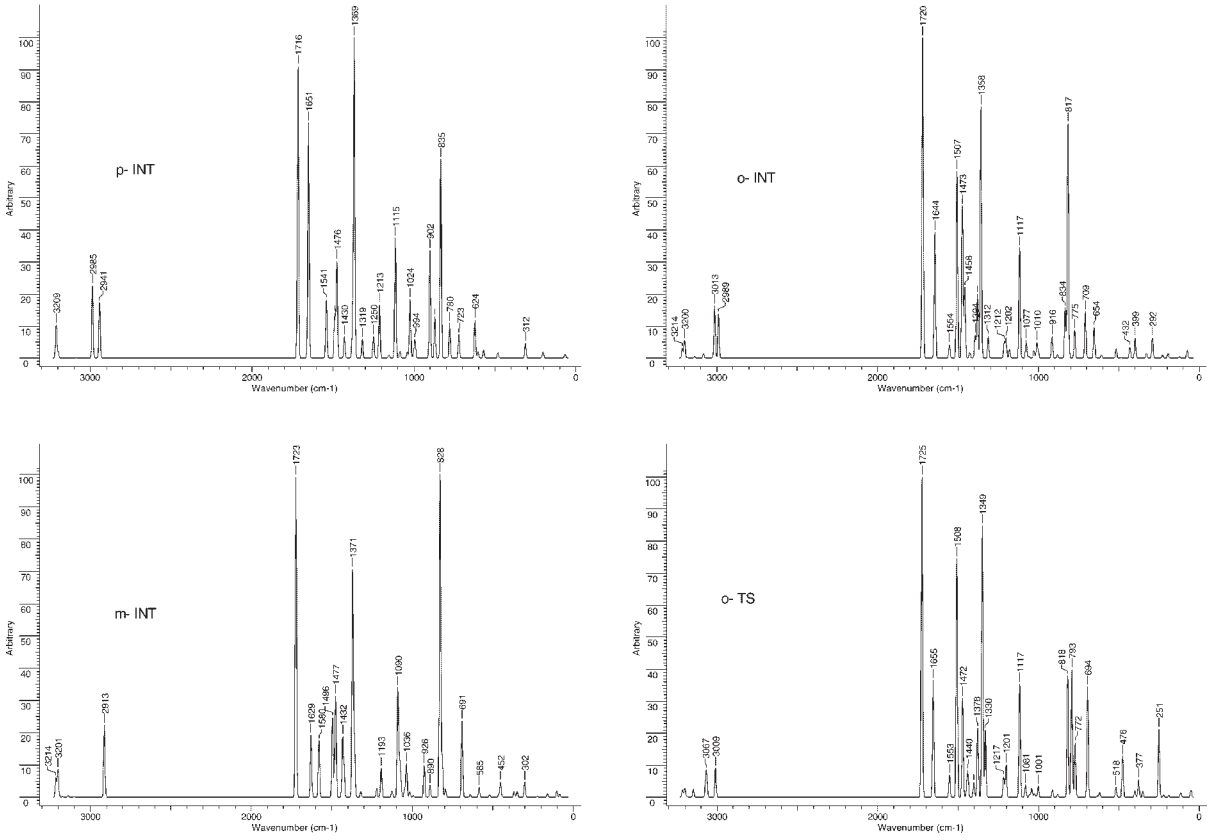

Figure 5. IR Spectra for three isomeric INTs and an *ortho* TS

It is worth noting that the stretching frequencies of both the C—H and C—N bonds in intermediates are stronger than that in transition states. Taking the spectra of *o*-INT and *o*-TS as an example, the C—H bond stretching frequencies there, $\sim 3000\,cm^{-1}$, are stronger than that in *o*-TS. Also, a slight red shift could be found for the C—H stretching frequencies on going from *o*-TS to *o*-INT. Meanwhile, a blue shift by $24\,cm^{-1}$ (from 793 to $817\,cm^{-1}$) could be found for the much sharper C—N stretch. The strong vibrational mode of the C—N bond in TS shows that the C—N bond has already been partly formed there. Also, its blue shift on going from TS to INT reflects that the C—N bond is becoming even stronger in the Wheland intermediate. In contrast, the slight red shift of the weak C—H stretch shows that the tetrahedral C—H bond is becoming weaker, but is not yet readily broken at the stage of forming the Wheland intermediate. Overall, the infrared spectra of both TS and INT support the contention that the formation of the C—N bond and the cleavage of the C—H bond are not concerted but proceed stepwise in the process of nitration, consistent with the experimental fact of the lack of a kinetic isotopic effect in most aromatic nitrations.

CONCLUSIONS

We have compared and discussed the nitration pathways, in particular the rate-limiting step of isomeric nitrations of toluene with the nitronium ion, with respect to the corresponding benzene case. Two functions played by the methyl group in the nitration of toluene have been deduced out by its inductive and superconjugative effect. One serves as the attacker by activating the *ortho* and *para* sites but deactivating the *meta* site, resulting in the kinetic order *para* > *ortho* > benzene > *meta*. Another acts in stabilizing the σcomplexes of toluene–NO_2^+, resulting in the thermodynamic stability order *p*-$ArCH_3$–NO_2^+ > *o*-$ArCH_3$–NO_2^+ > *m*-$ArCH_3$–NO_2^+ > PhH–NO_2^+. The infrared spectra by DFT calculations suggest that the nitration of toluene may follow the classical S_E2 mechanism.

Acknowledgments

We greatly appreciate the support of this work by the National Natural Science Foundation of China (No. 20173028). L. Chen also acknowledges a grant from the Science Center of Zhejiang University of Technology.

REFERENCES

1. Ingold CK. *Structure and Mechanism in Organic Chemistry.* Cornell University Press: Ithaca, NY, 1953.
2. Wheland GW. *J. Am. Chem. Soc.* 1942; **64**: 900–909.
3. Ebersonand L, Radner F. *Acc. Chem. Res.* 1987; **20**: 53–59.
4. Attina M, Cacace F, Yanez M. *J. Am. Chem. Soc.* 1987; **109**: 5092–5097.
5. Politzer P, Jayasuriya K, Sjoberg P, Laurence PR. *J. Am. Chem. Soc.* 1985; **107**: 1174–1177.
6. Morrison JD, Stanney K, Tedder JM. *J. Chem. Soc., Perkin Trans. 2* 1981; 967–969.
7. Gleghorn JT, Torossian G. *J. Chem. Soc., Perkin Trans. 2* 1987; 1303–1310.
8. Feng JK, Zhen XH, Zerner MC. *J. Org. Chem.* 1986; **51**: 4531–4536.
9. Szabo KJ, Hornfeldt A-B, Gronowitz S. *J. Am. Chem. Soc.* 1992; **114**: 6827–6834.
10. Szabo KJ, Hornfeldt A-B, Gronowitz S. *J. Am. Chem. Soc.* 1992; **114**: 6827–6834.
11. Eberson L, Hartshorn MP, Radner F. *Acta Chem. Scand.* 1994; **48**: 937–950.
12. Xiao HM, Chen LT, Ju XH. *Sci. China* 2003; **46**(5): 453–464.
13. Seminario JM, Politzer P. *Modern Density Functional Theory: A Tool for Chemistry.* Elsevier: Amsterdam, 1995.
14. Labanowski JK, Andzelm JW (eds). *Density Functional Methods in Chemistry.* Springer-Verlag: New York, 1991.
15. Sosa C, Lee C. *J. Chem. Phys.* 1993; **98**: 8004–8011.
16. Xiao HM, Chen ZX. *The Modern Theory of Tetrazole Chemistry.* Science Press: Beijing, 2000.
17. Zhang J, Xiao HM, Gong XD. *J. Phys. Org. Chem.* 2001; **14**: 583–588.
18. Xiao HM, Li JS, Dong HS. *J. Phys. Org. Chem.* 2001; **14**: 644–649.
19. Li JS, Xiao HM, Dong HS. *Chin. J. Chem.* 2000; **18**(6): 815–819.
20. Chen ZX, Xiao HM, Song WY. *J. Mol. Struct. (Theochem)* 1999; **460**: 167–173.
21. Gong XD, Xiao HM, Tian H. *Int. J. Quantum Chem.* 2002; **86**: 531–540.
22. Frisch MJ, Trucks GW, Schlegel HB, Scuseria GE, Robb MA, Cheeseman JR, Zakrzewski VG, Montgomery JA, Stratmann RE, Burant JC, Dapprich S, Millam JM, Daniels AD, Kudin KN, Strain MC, Farkas O, Tomasi J, Barone V, Cossi M, Cammi R, Mennucci B, Pomelli C, Adamo C, Clifford S, Ochterski J, Petersson GA, Ayala PY, Cui Q, Morokuma K, Malick DK, Rabuck AD, Raghavachari K, Foresman JB, Cioslowski J, Ortiz JV, Stefanov BB, Liu G, Liashenko A, Piskorz P, Komaromi I, Gomperts R, Martin RL, Fox DJ, Keith T, Al-Laham MA, Peng CY, Nanayakkara A, Gonzalez C, Challacombe M, Gill PMW, Johnson BG, Chen W, Wong MW, Andres JL, Head-Gordon M, Replogle ES, Pople JA. *Gaussian 98, Revision A.7*. Gaussian: Pittsburgh, PA, 1998.
23. Melander L. *Ark. Kemi* 1950; **2**: 211–292.
24. Lauer WM, Noland WE. *J. Am. Chem. Soc.* 1953; **75**: 3689–3692.
25. Becke AD. *J. Chem. Phys.* 1992; **97**: 9173–9177.
26. Becke AD. *J. Chem. Phys.* 1993; **98**: 5648–5652.
27. Scott AP, Radom L. *J. Phys. Chem.* 1996; **100**: 16502–16513.